SCIEPublish

Article

Nitrogen-controlled Valorization of Xylose-derived Compounds by Metabolically Engineered *Corynebacterium glutamicum*

Lynn S. Schwardmann, Marielle Rieks, Volker F. Wendisch *

Genetics of Prokaryotes, Faculty of Biology and CeBiTec, Bielefeld University, Universitätsstr. 25, 33615 Bielefeld, Germany; l.schwardmann@uni-bielefeld.de (L.S.S.); marielle.rieks@uni-bielefeld.de (M.R.)

* Corresponding author. E-mail: volker.wendisch@uni-bielefeld.de (V.F.W.)

Received: 4 May 2023; Accepted: 25 May 2023; Available online: 31 May 2023

ABSTRACT: The implementation of bioprocesses in an economically feasible and industrial competitive manner requires the optimal allocation of resources for a balanced distribution between biomass formation and product synthesis. The decoupling of growth and production in two-stage bioprocesses, aiming to ensure sufficient growth before the onset of production, is particularly relevant when target products inhibit growth. In order to avoid expensive inducer molecules, continuing process monitoring, elaborate individual process optimization, and strain engineering, we developed and applied nitrogen deprivation-induced expression of genes for product biosynthesis. Two native nitrogen deprivation-inducible promoters were identified and shown to function for dynamic growth-decoupled gene expression or CRISPRi-mediated gene knockdown in *C. glutamicum* with superior induction factors than the standard IPTG-inducible P_{trc} promoter. Valorization of xylose to produce either the sugar acid xylonic acid or the sugar alcohol xylitol from xylose as sole source of carbon and energy was demonstrated. Competitive titers of up to 34 $g \cdot L^{-1}$ xylonate and 13 $g \cdot L^{-1}$ xylitol were achieved in two-stage processes. We discussed that the transfer to bioprocesses with *C. glutamicum* using carbon sources other than xylose appears straightforward in particular regarding production of growth-inhibitory compounds by their growth-decoupled fermentative production.

Keywords: Two-stage bioprocess; Nitrogen starvation; *Corynebacterium glutamicum*; Xylitol; Xylonate; CRISPRi; Sustainable production; Xylose

1. Introduction

In the context of a sustainable, future-oriented bioeconomy, lignocellulose, which is considered the most abundant biomass, presents an attractive second-generation feedstock with an estimated annual production of 182 billion tons [1]. Besides glucose, lignocellulosic hydrolysate mostly contains xylose (15–37%) as monomeric sugar [2], making its valorization into xylose-derivable valuable compounds highly interesting. The sugar alcohol xylitol and the sugar acid xylonate belong to this compound class.

Generally, sugar acids are used as chemical intermediates. D-gluconate, the best known one, reached an annual production of 90 000 tons worldwide in 2009 [3]. It is industrially produced by oxidation of the monosaccharide glucose [3] and thus competes with its use in human and animal nutrition. Due to similar physical properties, xylonate, which can be derived from the non-food sugar xylose, represents a highly interesting substitute [4]. Xylonate has found applications as dispersing agent for cement and concrete [5], clarifying agent for polyolefins [6], precursor in the production of co-polyamides [7] or therapeutically active compounds [8] and the synthesis of 1,2,3-butanetriol [9] or 3,4-dihydroxybutyrate [10]. Chemical synthesis of xylonate is known, but characterized by low selectivity [11]. This obstacle can be overcome by the high efficiency of microbial conversion of xylose into xylonic acid, which proceeds via xylose or glucose dehydrogenase-mediated oxidation to xylonolactone, followed by lactonase-catalyzed or spontaneous hydrolysis to xylonate [12], as exemplified for native producer organisms, e.g., *Pseudomonas fragi* [13], *Klebsiella pneumoniae* [14], *Paraburkholderia sacchari* [15] and *Gluconobacter oxydans* [16], as well as genetically engineered strains of *Escherichia coli* [17], *Corynebacterium glutamicum* [18], and *Saccharomyces cerevisiae* [4].

Xylitol, a five-carbon sugar alcohol naturally occurring in vegetables, fruits and hardwood trees like birch and beechwood has gained popularity as artificial non-diabetic sweetener in nutrition and has reached a market size of almost 9 million US dollars in 2021 [19]. Besides, it is used in the pharmaceutical industry for its insulin-independent metabolism, anti-cariogenic and calcium absorption-facilitating properties [20]. The platform compound xylitol has the potential as precursor for production of propylene glycol, poly(ethylene glycol), glycerol, xylaric acid or lactic acid [21]. Since only low xylitol concentrations are found in natural sources [21], either chemical synthesis via catalytic hydrogenation of lignocellulosic biomass using toxic catalysts, high pressure

https://doi.org/10.35534/sbe.2023.10009

and energy [21], or biotechnological production is required [22]. Biosynthesis of xylitol as part of xylose metabolism is widespread among yeast and fungi via NADPH-dependent reduction of xylose by xylose reductase (Xr) [23], but only few bacterial species, including corynebacteria [24] were reported to show slow xylitol formation, e.g., the isolate *Corynebacterium* sp. No. 208 accumulated 69 $g \cdot L^{-1}$ of D-xylitol in 14 days [24]. Consequently, biotechnological production approaches are centered on yeast, particularly the genus *Candida* [25], but have also been extended to established biotechnological workhorses, including *C. glutamicum* [26].

C. glutamicum is primarily known for amino acid production in the million ton scale [27]. Among others, its reputation as versatile chassis is endowed with high stress tolerance and robustness [28,29], the absence of endotoxins [30], and the suitability for the production of GRAS status compounds [31], such as sugars, sugar alcohols [32,33], the flavor enhancer L-glutamate [34], and other amino acids as well as related compounds [35,36]. By synthetic biology, the product spectrum is further expanded to diamines [37], vitamins [38], organic acids [39], and alcohols [40]. Biobased production with *C. glutamicum* benefits from the naturally broad carbon spectrum and the access to non-native sugars is achieved by the introduction of synthetic pathways [41].

A detailed understanding of the metabolism of macronutrients has been gained, e.g., regarding nitrogen metabolism. Genetic regulation of nitrogen metabolism involves the global repressor protein AmtR, which mediates the nitrogen-dependent regulation of genes for ammonium transporters, proteins for ammonium assimilation and signal transduction, urea and creatinine metabolism, but also some uncharacterized ones [42,43]. Upon nitrogen limitation, repression is released by interaction of AmtR with the adenylated signal transduction protein GlnK [43]. Two promoters of the operons *amtB-glnK-glnD* and *amtA-ocd-soxA* were reported to show the strongest and fastest response to nitrogen-limiting conditions [42], making them interesting options for auto-induction. The most common induction strategies rely on the addition of exogenous inducer molecules such as isopropyl β-D-thiogalactoside (IPTG). Besides the fact that induction at the intended cell density must be the precisely timed, the high costs for inducers (IPTG, lactose, galactose, gentiobiose, fucose, lactitol or sucralose [44]) make their addition economically unattractive in industrial scale and the toxicity may preclude their use in the production of pharmaceuticals [45]. As alternative, completely inducer-free dynamic pathway regulation by auto-induction has been developed, in which growth and production phases may be decoupled. During the second phase of such two-stage processes, non-growing stationary phase cells can maintain their metabolic activity, which enables the predominant allocation of resources to the product formation for high protein yields [46]. Moreover, stationary phase cells tend to be more robust and stress resistant than exponentially growing ones [47]. Most developed auto-induction systems make use of carbon catabolite repression, metabolite regulated promoters and biosensors, or employ quorum sensing [48,49]. All of these build on natural dynamic regulation mechanisms, which ensure the maintenance of pathway balances under varying environmental conditions, but simultaneously render them innately highly sensitive and require elaborate product-, strain-, and process-specific calibration [50–52]. Moreover, the type of the carbon source can affect the regulatory network which entails severe and often unpredictable changes in cellular metabolism [53], and it is not suited for the synthesis of molecules with carbohydrate backbones. Unlike most model microorganisms with pronounced carbon catabolite repression, *C. glutamicum* naturally co-utilizes different carbohydrates [29]. Therefore, a dependency from macronutrients other than the carbon source in combination with respective responsive promoters provides an interesting alternative [53,54], but has not been studied for *C. glutamicum*. Here, we describe auto-induction for nitrogen-controlled production of sugar acid xylonate and sugar alcohol xylitol from pentose xylose by metabolically engineered *C. glutamicum*.

2. Materials and Methods

2.1. Bacterial Strains and Cultivation Conditions

All strains used in this study are listed in Table 1 and all plasmids are given in Table 2. *E. coli* DH5α [55] served as host for plasmid construction, amplification, and maintenance. Cultures were grown at 37 °C and 180 rpm in baffled shake flasks in lysogeny broth (LB), supplemented with antibiotics (100 $\mu g \cdot mL^{-1}$ spectinomycin, 100 $\mu g \cdot mL^{-1}$ ampicillin, 10 $\mu g \cdot mL^{-1}$ tetracycline, 30 $\mu g \cdot mL^{-1}$ chloramphenicol), according to the plasmids.

Cultures of *C. glutamicum* were grown in baffled shake flasks at 30 °C and 120 rpm on a rotary shaker, supplemented with appropriate antibiotics (5 $\mu g \cdot mL^{-1}$ tetracycline, 7 $\mu g \cdot mL^{-1}$ chloramphenicol). Precultures were grown in LB, harvested by centrifugation (3200× *g*, 7 min), washed and resuspended in CgXII lacking the accessible nitrogen sources $(NH_4)_2SO_4$ and urea for inoculum of main cultures. Main cultures were grown in CgXII minimal medium with regular nitrogen content (CgXII, [56]) and 40 $g \cdot L^{-1}$ glucose or xylose as carbon source. To limit biomass formation while maintaining xylitol or xylonate production, a medium with reduced accessible nitrogen content (N-CgXII, containing 5% nitrogen in form of 1 $g \cdot L^{-1}$ $(NH_4)_2SO_4$ and 0.25 $g \cdot L^{-1}$ urea instead of 20 $g \cdot L^{-1}$ $(NH_4)_2SO_4$ and 5 $g \cdot L^{-1}$ urea) was chosen. Production experiments were performed in 10 mL in baffled shake flasks for 144 h as at that time we assumed that production has terminated either by exhaustion of the carbon source xylose or by product inhibition. It has to be noted that the volumetric productivity may be increased by optimizing the production time towards shorter incubation. Growth was monitored by optical density at 600 nm (OD_{600}) in a V-1200 Spectrophotometer (VWR, Radnor, PA, USA) and the previously determined factor of 0.25 $g \cdot L^{-1}$ cell dry weight (CDW) was assumed to correspond to an OD_{600} of 1.

To investigate the effect of xylitol presence on growth, cells were cultivated in a BioLector microcultivation system (m2p-labs, Aachen, Germany) in a volume of 1 mL in a 48-well flower plates at 30 °C, 85% humidity and a shaking frequency of 1100 rpm. Growth was monitored by backscatter light signal at 620 nm. Gene expression from pECXT99A derived plasmids and sgRNA expression from pS_dCas9 derived plasmids was induced by the addition of 1 mM isopropyl-β-D-1-thiogalactopyranoside (IPTG). Additionally, 0.25 $\mu g \cdot mL^{-1}$ anhydrotetracycline (aTc) was added for dCas9 expression from pS_dCas9-*gfp*$_{UV}$.

Table 1. List of strains used in this study.

Strain	Relevant Characteristics	Source
E. coli DH5α	*E. coli* F-Φ80*lacZ*ΔM15 Δ(*lacZYA-argF*) U169 *endA1 recA1 hsdR17* (rK^-, mK^+) *supE44 thi-1 gyrA96 relA1 phoA*	[55]
C. glutamicum WT	*C. glutamicum* wild-type, ATCC13032	[57]
WT-EV	*C. glutamicum* WT carrying pECXT_P$_{syn}$	[58]
gX	*C. glutamicum* ATCC 13032 derivate with the synthetic operon, consisting of *xylA* of *Xanthomonas campestris* and *xylB* of *C. glutamicum* WT, integrated into the gene locus *actA* (cg2840)	[59]
gX-EV	*C. glutamicum* gX, carrying pECXT99A	This study
gX-P$_{trc}$-*xr*	*C. glutamicum* gX, carrying pECXT99A-*xr*$_{R.m}$	This study
gX-P$_{amtA}$-*xr*	*C. glutamicum* gX, carrying pECXT_P$_{amtA}$-*xr*$_{R.m}$	This study
gX-P$_{amtB}$-*xr*	*C. glutamicum* gX, carrying pECXT_P$_{amtA}$-*xr*$_{R.m}$	This study
gX-P$_{trc}$-*xylB*	*C. glutamicum* gX, carrying pECXT99A-*xylB*$_{C.c.}$	This study
gX-P$_{amtA}$-*xylB*	*C. glutamicum* gX, carrying pECXT_P$_{amtA}$-*xylB*$_{C.c.}$	This study
gX-P$_{amtB}$-*xylB*	*C. glutamicum* gX, carrying pECXT_P$_{amtB}$-*xylB*$_{C.c.}$	This study
WT-P$_{amtA}$-*gfp*	*C. glutamicum* WT, carrying pS_P$_{amtA}$-*gfp*$_{UV}$	This study
WT-P$_{amtB}$-*gfp*	*C. glutamicum* WT, carrying pS_P$_{amtB}$-*gfp*$_{UV}$	This study
WT-*gfp*	*C. glutamicum* WT, carrying pECXT_P$_{syn}$-*gfp*$_{UV}$	This study
WT-*gfp*-dCas9	*C. glutamicum* WT, carrying pECXT_P$_{syn}$-*gfp*$_{UV}$ and pS_dCas9-*gfp*$_{UV}$	This study
WT-*gfp*-P$_{amtA}$-dCas9	*C. glutamicum* WT, carrying pECXT_P$_{syn}$-*gfp*$_{UV}$ and pS_P$_{amtA}$-dCas9-*gfp*$_{UV}$	This study
WT-*gfp*-P$_{amtB}$-dCas9	*C. glutamicum* WT, carrying pECXT_P$_{syn}$-*gfp*$_{UV}$ and pS_P$_{amtB}$-dCas9-*gfp*$_{UV}$	This study

Table 2. List of plasmids used in this study.

Plasmids	Relevant Characteristics	Source
pK19*mobsacB*	Km^R, *E. coli/C. glutamicum* shuttle vector for construction of *C. glutamicum* deletion and insertion mutants (pK18 *ori*V$_{E.c.}$, *sacB*, *lacZα*)	[60]
pECXT99A	Tet^R, P$_{trc}$ lacI^q, pGA1 *ori*V$_{Cg}$, *C. glutamicum/E. coli* expression shuttle vector	[61]
pECXT_P$_{syn}$-*gfp*$_{UV}$	pECXT_P$_{syn}$ derivative for constitutive expression of *gfp*$_{UV}$	[58]
pMA-RQ_XR_*R-mucilaginosa*	Amp^R, cloning plasmid with sequence of codon-harmonized version of xylose reductase from *Rhodotorula mucilaginosa* NBT11	synthesized by Geneart AG, Regensburg, Germany
pECXT99A-*xr*$_{R.m.}$	pECXT99A derivate for IPTG-inducible expression of *xr* from *Rhodotorula mucilaginosa* NBT11 (*xr*$_{R.m}$)	This study
pECXT_P$_{amtA}$-*xr*$_{R.m.}$	pECXT99A derivative for nitrogen-starvation inducible expression of *xr*$_{R.m.}$ by P$_{amtA}$	This study
pECXT_P$_{amtB}$-*xr*$_{R.m.}$	pECXT99A derivative for nitrogen-starvation inducible expression of *xr*$_{R.m.}$ by P$_{amtB}$	This study
pEKEx3_*xylXABCD*$_{C.c.}$	$Spec^R$; pEKEx3 derivative for the regulated expression of *xylXABCD*Cc of *Caulobacter crescentus*	[18]
pECXT99A-*xylB*$_{C.c.}$	pECXT99A derivative for IPTG-inducible expression of *xylB* of *Caulobacter crescentus* (*xylB*$_{C.c}$)	This study
pECXT_P$_{amtA}$-*xylB*$_{C.c.}$	pECXT99A derivative for nitrogen-starvation inducible expression of *xylB*$_{C.c.}$ by P$_{amtA}$	This study
pECXT_P$_{amtB}$-*xylB*$_{C.c.}$	pECXT99A derivative for nitrogen-starvation inducible expression of *xylB*$_{C.c.}$ by P$_{amtB}$	This study
pECXT_P$_{syn}$-*gfp*$_{UV}$	TetR, pECXT99A derivative for constitutive expression from promoter P$_{syn}$	This study
pS_dCas9	anhydrotetracycline-inducible expression of dCas9 from *Streptococcus pyogenes* and IPTG-inducible expression of the dCas9 handle	[62]
pS_dCas9-*gfp*$_{UV}$	pS_dCas9 plasmid carrying the *gfp*$_{UV}$ sgRNA	This study
pS_P$_{amtA}$-dCas9-*gfp*$_{UV}$	pS_dCas9-*gfp*$_{UV}$ derivative with P$_{tetA}$ replaced by P$_{amtA}$ for P$_{amtA}$-regulated CRISPRi-mediated repression of *gfp*$_{UV}$	This study
pS_P$_{amtB}$-dCas9-*gfp*$_{UV}$	pS_dCas9-*gfp*$_{UV}$ derivative with P$_{tetA}$ replaced by P$_{amtB}$ for P$_{amtB}$-regulated CRISPRi-mediated repression of *gfp*$_{UV}$	This study
pS_P$_{amtA}$-*gfp*$_{UV}$	pS_P$_{amtA}$-dCas9-*gfp*$_{UV}$ derivative with dCas9 replaced by *gfp*$_{UV}$ for P$_{amtA}$-regulated expression of *gfp*$_{UV}$	This study
pS_P$_{amtB}$-*gfp*$_{UV}$	pS_P$_{amtB}$-dCas9-*gfp*$_{UV}$ derivative with dCas9 replaced by *gfp*$_{UV}$ for P$_{amtB}$-regulated expression of *gfp*$_{UV}$	This study

2.2. Molecular Genetic Methods

Promoter and gene sequences were amplified with ALLin^{TM} HiFi DNA Polymerase (highQu GmbH, Kraichtal, Germany) and the listed oligonucleotides (Table S1, obtained from Metabion, Planegg/Steinkirchen, Germany).

The promoter sequences of *amtA* (P$_{amtA}$) and *amtB* (P$_{amtB}$), spanning approximately 300 nucleotides of the 5′ sequence adjacent to the respective start codon were amplified from genomic DNA of *C. glutamicum* WT [57], which was isolated as described previously [63]. Promoter-less genes *gfp*$_{UV}$, *xylB* and *xr* were amplified from plasmids pECXT_P$_{syn}$-*gfp*$_{UV}$, pEKEx3_*xylXABCD*, and pMA-RQ_XR_*R-mucilaginosa*, respectively. Primer overhangs were used for integration of a consensus ribosome binding site (RBS) sequence (GAAAGGAGGCCCTTCAG) in front of *gfp*$_{UV}$ and *xylB*, whereas an optimized RBS (CCCGAAAAGTCGAAAGGAGGTATTTTA, designed using the Salislab software, [64]), was included in front of *xr*.

A single guide RNA (sgRNA) of 20 nt, homologous to the non-template strand of *gfp*$_{UV}$, was designed with the CRISPy-webtool [65], based on the genome sequence of *C. glutamicum* WT [57] and single-stranded oligonucleotides were used to attain the double-stranded sgRNA insert by oligo annealing, as described elsewhere [62]. All restriction enzymes were obtained from NEB (NEB, Frankfurt, Germany). pS_dCas9 was linearized with PstI for insertion of the sgRNA. pS_dCas9-*gfp*$_{UV}$ was cut with AatII and BglII for promoter replacement and resulting plasmids pS_dCas9_P$_{xxx}$-*gfp*$_{UV}$ were cut with BglII and PspXI for replacement of the dCas9 gene for *gfp*$_{UV}$. pECXT99A was linearized using BamHI alone or in combination with NdeI for integration

of a gene or for simultaneous promoter replacement, respectively. All linearized plasmids were dephosphorylated (Antarctic phosphatase, New England Biolabs, Frankfurt, Germany) before plasmid assembly by the method of Gibson [66].

A V-1200 Spectrophotometer (VWR, Radnor, PA, USA) was used to determine DNA concentrations and the sequences of all inserts of newly constructed plasmids were verified by sequencing and transformants confirmed by colony PCR with respective oligonucleotides (Table S1). A plasmid miniprep kit (GeneJET, Thermo Fisher Scientific, Schwerte, Germany) and a PCR and gel extraction kit (Macherey-Nagel, Düren, Germany) were used for plasmid isolation and purification of DNA sequences, respectively. Standard molecular genetic techniques were performed according to previously described procedures [67]. *E. coli* competent cells were prepared by the $CaCl_2$ method [67] for transformation by heat shock at 42 °C [56], while *C. glutamicum* cells were transformed by electroporation, followed by heat shock at 46 °C [56].

2.3. Flow Cytometry for Fluorescence Analysis and Quantification

The fluorescence of Gfp_{UV} was analyzed using flow cytometry (flow cytometer Gallios™, Beckman Coulter, Krefeld, Germany) with excitation by a blue solid-state laser at 405 nm and detection by a 525/50 nm bandpass filter. The forward-(FSC) and side-scatter (SSC) signals were measured for 20,000 cells per sample. Samples for analysis of induction or knockdown of gfp_{UV} expression were taken after 24 h, diluted to an OD_{600} of approximately 0.1 in TN buffer (50 mM Tris-HCl, 50 mM NaCl, pH 6.3) and analyzed immediately with WT-EV cells as reference to adjust for autofluorescence.

2.4. Enzymatic Activity Assays

For analysis of xylose reductase or xylose dehydrogenase activity, cells were grown in 50 mL CgXII or N-CgXII, supplemented with 40 $g \cdot L^{-1}$ xylose in baffled shake flasks for 68 h. When indicated, 1 mM IPTG was added and cultivation started for gX-P_{trc}-*xylB* or of gX-P_{trc}-*xr*, when an OD_{600} of 4 was reached to permit sufficient biomass formation despite xylitol cytotoxicity. All following steps were performed at 4 °C or on ice. Cells were harvested by centrifugation (20,200× *g*, 7 min), washed three times in resuspension buffer (50 mM Tris HCl, pH 7.5), resuspended in 2 mL, and disrupted by ultrasonication (UP 200S, Dr. Hielscher GmbH, Teltow, Germany) at 60% amplitude and a 0.5 s pulsing cycle for 9 min. The method of Bradford was employed for quantification of total crude protein concentrations with bovine serum standard as reference [68]. Measurements of enzymatic activity were performed within 48 h after cell lysis.

Both assays were performed in 1 mL total volume at 30 °C, using crude extracts containing >1 $g \cdot L^{-1}$ total protein. Absorbance was followed for 3 min in a photometer (Shimadzu UV-1650 PC photometer, Shimadzu, Duisburg, Germany) at 340 nm before and after the start of the reaction by xylose addition. Specific activities, given in units per mg of total protein ($U \cdot mg^{-1}$), were calculated with one unit corresponding to the conversion of 1 µmol NADPH or NAD^+ per min under the described conditions. Xylose reductase activity was determined as described elsewhere [26] with a final sample composition of 100 mM potassium phosphate (pH 6.0) reaction buffer, 0.2 mM NADPH, and 200 mM xylose. Xylose reductase activity was determined as described elsewhere [69] with a final sample composition of 50 mM sodium phosphate (pH 8) reaction buffer, 2 mM NAD, and 200 mM xylose.

2.5. Product and Substrate Quantification

2.5.1. HPLC Analysis

Substrate and products were quantified by high performance liquid chromatography (HPLC) with an Agilent 1200 series system (Agilent Technologies Deutschland GmbH, Böblingen, Germany), equipped with an amino exchange column (Aminex, 300 × 8 mm, 10 µm particle size, 25 Å pore diameter, CS Chromatographie Service, Langerwehe, Germany). Compounds were separated under isocratic conditions at a flow rate of 0.8 $mL \cdot min^{-1}$ for 17 min with 5 mM H_2SO_4 as mobile phase. Xylose and xylitol were detected by the refractive index signal (RID G1362A, 1200 series, Agilent Technologies, Böblingen, Germany) and xylonate by a diode array detector (DAD G1315B, 1200 series, Agilent Technologies) at 210 nm. Samples were taken at indicated time points, centrifuged (20,200× *g*, 15 min) and stored at −20 °C until analysis.

2.5.2. Spectrophotometric Xylose Quantification

Coelution of xylose and xylonate under the applied conditions prohibited their differentiation and quantification by RID detection alone. For clear compound identity, xylonate was exclusively quantified via the DAD signal, while the xylose content of culture supernatants was determined using a D-xylose assay kit (Megazyme Ltd., Wicklow, Ireland).

2.5.3. Data Analysis and Presentation

Statistical significance of triplicate cultivations or measurements was determined by the two-sided unpaired Student's t-tests with *p*-values of <0.001 (***); $p < 0.01$ (**); $p < 0.05$ (*) and $p \geq 0.05$ (n.s.: not significant). Values of biomass formation and product synthesis were adjusted to volume reduction due to evaporation.

3. Results

3.1. Characterization of Nitrogen-dependent Promoters for Nitrogen Starvation-induced Gene Expression

Transcription of the operons *amtB-glnK-glnD* and *amtA-ocd-soxA* is known to be induced upon nitrogen limitation. The promoter sequences of *amtA* and *amtB*, referred to as P_{amtA} and P_{amtB}, were amplified as 314 and 284 bp fragments from the genome of C. *glutamicum* WT and included the two contained AmtR consensus binding motifs (**A T C T A T A G** A A C G **A T A G**), located -97 to -86 and -61 to -46 of *amtA* and -186 to -159 and -118 and -91 of *amtB* start codons, respectively [42].

Prior to establishing nitrogen content-dependent production of value-added compounds, the promoter-less gene of the green fluorescent protein (Gfp_{UV}) was harnessed as reporter for initial investigation of the candidate promoters P_{amtA} and P_{amtB}. P_{amtA}-or P_{amtB}-controlled gfp_{UV} expression was attained by construction of the plasmids pS_P_{amtA}-gfp_{UV} and pS_P_{amtB}-gfp_{UV}, which were used to transform *C. glutamicum* WT, yielding strains WT-P_{amtA}-gfp_{UV} and WT-P_{amtB}-gfp_{UV}. Standard CgXII minimal medium, which is optimized for nitrogen-demandin g·lysine biosynthesis, contains 468 mM of accessible nitrogen in the form of urea and ammonium sulfate (CgXII). Here, we used a nitrogen-limiting medium named N-CgXII with accessible nitrogen reduced to 5% (23 mM; see Materials and Methods). The cultivation of WT-P_{amtA}-gfp_{UV} and WT-P_{amtB}-gfp_{UV} for 24 h in N-CgXII instead of CgXII decreased the total attainable biomass concentration to approximately 25%. Hence, the nitrogen content in N-CgXII was suited to set nitrogen-limiting growth conditions and the Gfp_{UV} fluorescence of these cells, measured by flow cytometry, was used to analyze the response of P_{amtA} and P_{amtB}.

The flow cytometry scatter plots showed a clear shift of the cell population to higher fluorescence intensities when N-CgXII was used instead of CgXII (representatively shown for P_{amtA} Figure 1A), confirming nitrogen starvation-induced gfp_{UV} expression. With the mean population fluorescence intensity serving as a measure for quantitative comparison of promoter strengths, approximately 18- and 5-fold increased expression was observed when strains WT-P_{amtA}-gfp_{UV} and WT-P_{amtB}-gfp_{UV} were cultivated with reduced nitrogen content as compared to regular CgXII medium nitrogen content (Figure 1C). Upon serial transfer from nitrogen liming cultivation to a second batch cultivation under nitrogen limitation, strains WT-P_{amtA}-gfp_{UV} and WT-P_{amtB}-gfp_{UV} showed approximately 11- and 7-fold higher expression than those after cultivation in CgXII (Figure 1C). Thus, to elicit nitrogen limitation and reporter gene induction in strains WT-P_{amtA}-gfp_{UV} and WT-P_{amtB}-gfp_{UV}, a single transfer from CgXII medium to N-CgXII medium was sufficient (Figure 1C).

3.2. Characterization of Nitrogen Starvation-induced CRISPRi Gene Repression

Conditional gene expression may depend, *i.a.*, on positive or negative control. On the basis of nitrogen limitation induced positive control of gfp_{UV} expression using promoters P_{amtA} and P_{amtB}, we aimed to demonstrate the general validity and applicability of this response to CRISPRi-mediated gene repression [70]. In this approach, CRISPRi served to invert the positive to a negative regulatory output. First, P_{amtA}- or P_{amtB}-controlled dCas9 expression was realized in plasmids pS_P_{amtA}-dCas9-gfp_{UV} or pS_P_{amtB}-dCas9-gfp_{UV} and compared to anhydrotetracyclin (aTc)-inducible dCas9 expression from promoter $P_{tetR/A}$ in plasmid pS_dCas9-gfp_{UV} as a reference. The gfp_{UV}-specific sgRNA was expressed from a second compatible plasmid named pECXT_P_{syn}-gfp_{UV}. The resulting strains were called WT-P_{amtA}-dCas9-gfp_{UV}, WT-P_{amtB}-dCas9-gfp_{UV} and WT-dCas9-gfp_{UV}. The addition of IPTG to all cultures at the beginning of the cultivation assured the expression of the gfp_{UV}-specific sgRNA and therefore rendered the knockdown dependent on expression of the gene encoding the complex's second component, the dCas9 protein.

Induction of $P_{tetR/A}$-controlled dCas9 expression by aTc addition decreased the fluorescence intensity of cells grown in CgXII to 27% (Figure 1D) and verified the functionality of the CRISPRi design. In the absence of aTc, repression of gfp_{UV} was neither observed with 100% nor with 5% nitrogen (Figure 1D and data not shown). By contrast, after two cultivations under nitrogen limiting conditions, cells of strains WT-P_{amtA}-dCas9-gfp_{UV} and WT-P_{amtB}-dCas9-gfp_{UV} showed CRISPRi-mediated repression of gfp_{UV} to 35% for P_{amtA} and 40% for P_{amtB}, respectively, as compared to cultivation with 100% nitrogen (Figure 1B,D). Unlike the positive control of gfp_{UV} expression using promoters P_{amtA} and P_{amtB} observed in the first nitrogen-limited cultivation (Figure 1C), CRISPRi-mediated repression of gfp_{UV} was only observed after transfer to a second nitrogen-limited cultivation (Figure 1D). This time delay may be attributed to the high stability of Gfp_{UV} [71] that requires dilution by cell division before repressed gfp_{UV} expression becomes detectable.

In summary, the nitrogen content-dependent response of both promoters is suitable for gene expression and CRISPRi-mediated repression in synthetic constructs without discernible basal expression and allows tight nitrogen content-dependent regulation with faster and higher response of P_{amtA}.

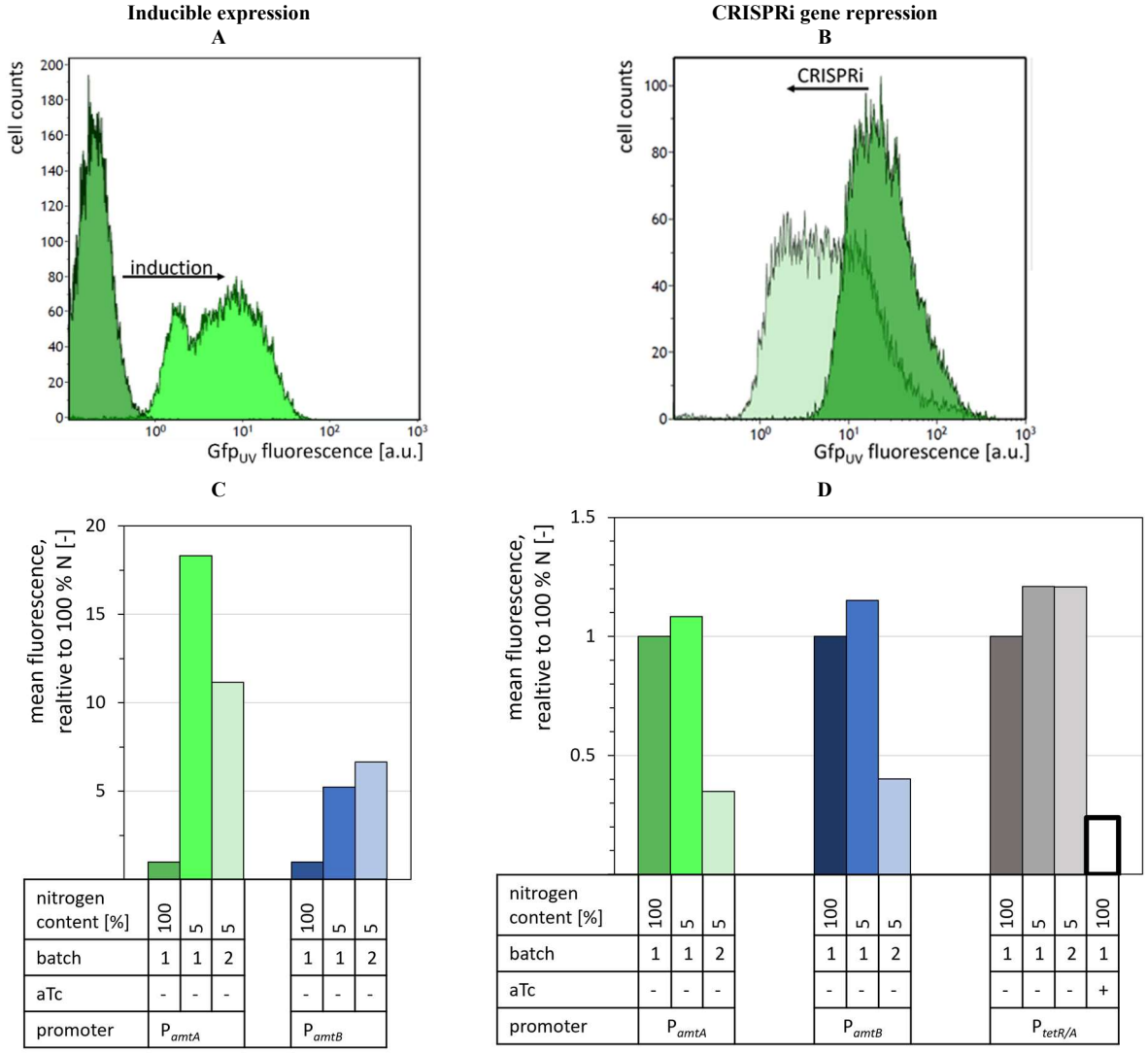

Figure 1. Characterization of nitrogen limitation inducible gene expression (**A**,**C**) and CRISPRi-mediated gene repression (**B**,**D**). Promoters P_{amtA} (green), P_{amtB} (blue) or aTc-inducible $P_{tetR/A}$-dCas9 (grey) were fused either to promoterless *gfp*UV (**A**,**C**) or to the dCas9 gene (**B**,**D**). IPTG (1 mM) was used to induce *gfp*UV-specific sgRNA expression in all CRISPRi cultivations. Cultivations were performed using the regular medium CgXII (100% nitrogen; dark blue, green, or grey) or N-CgXII containing 5% nitrogen for a single batch cultivation (intermediate green, blue or grey) or two consecutive batch cultivations (light green, blue, or grey) for 24 h. GfpUV fluorescence was analyzed by flow cytometry. Representative scatter plots depict the shifted fluorescence intensities of cells with P_{amtA}-induced GfpUV expression after one batch cultivation in N-CgXII (**A**) and for CRISPRi knockdown after two batch cultivations in N-CgXII (**B**). Relative mean fluorescence was normalized to the respective non-induced state. As positive control, $P_{tetR/A}$-controlled dCas9 expression was induced with 0.25 µg·mL^{-1} aTc (white box in **D**).

3.3. Nitrogen-limitation Induced Expression of Heterologous Genes for Xylose Reductase and Xylose Dehydrogenase

Based on our prior work on xylitol and xylonate production by recombinant *C. glutamicum* [18,72], the genes *xylB* encoding xylose dehydrogenase from *Caulobacter crescentus* and *xr* coding for xylose reductase from *Rhodotorula mucilaginosa* NBT11 were chosen for expression in strain gX. This xylose-utilizing strain is characterized by the genomic integration of the synthetic xylose utilization operon for production of xylose isomerase from *Xanthomonas campestris* and native xylulokinase [73]. Genes *xylB* and *xr* were cloned under the control of nitrogen limitation-inducible promoters P_{amtA} and P_{amtB} or IPTG-inducible P_{trc}, yielding the xylonate producer strains gX-P_{trc}-*xylB*, gX-P_{amtA}-*xylB*, gX-P_{amtB}-*xylB*, and the xylitol producer strains gX-P_{trc}-*xr*, gX-P_{amtA}-xr, gX-P_{amtB}-*xr*. As negative control, gX was transformed with the empty vector and called gX-EV.

Functional expression of xylose dehydrogenase and xylose reductase genes was examined by enzyme activity assays (Figure 2A,B). As expected, crude extracts of the empty vector control strain and each strain cultivated under non-inducing conditions lacked detectable xylose dehydrogenase and xylose reductase activities (Figure 2A,B). Induction of the xylose dehydrogenase gene was evident for strain gX-P_{trc}-*xylB* in the presence of IPTG and led to activities of 9.8 ± 1.4 and 10.1 ± 0.9 U·mg^{-1} in regular CgXII medium and nitrogen-limited medium N-CgXII, respectively (Figure 2A). Nitrogen-starvation induction was observed for strains gX-P_{amtA}-*xylB* and gX-P_{amtB}-*xylB,* leading to xylose dehydrogenase activities of 3.4 ± 0.7 U·mg^{-1} and 0.7 ± 0.1 U·mg^{-1}, respectively, under nitrogen-limiting conditions (Figure 3A). Similarly, nitrogen-limiting conditions also induced xylose reductase in strains gX-P_{amtA}-xr

and gX-P_{amtB}-*xr* to reach 0.5 ± 0.1 U·mg^{-1} and 0.7 ± 0.1 U·mg^{-1}, respectively (Figure 2B). Thus, functional expression of xylose reductase and xylose dehydrogenase with P_{amtA} or P_{amtB} is dynamically controllable by the prevalent nitrogen availability and provides a promising basis for exploitation of these promoters for nitrogen content-controlled production of xylitol and xylonate.

In the case of IPTG-controlled xylose reductase gene expression, we noted that IPTG addition at inoculation completely impeded growth of strain gX-P_{trc}-*xr* (data not shown). This indicated that xylitol production from xylose impairs growth with xylose of strain gX as previously observed for addition of xylitol to other *C. glutamicum* strains [74]. Indeed, when addition of IPTG was delayed to the mid-exponential growth phase at a biomass concentration of 1 g·L^{-1}, xylose reductase activities of 0.5 ± 0.1 and 0.5 ± 0.1 U·mg^{-1} could be measured using both CgXII and N-CgXII media.

As xylitol is known to perturb the propagation of various microorganisms including *C. glutamicum*, gX was cultivated in CgXII with 40 g·L^{-1} glucose or xylose as sole carbon and energy source in the presence of different xylitol concentrations. Growth with xylose was severely inhibited by xylitol as reflected by reduced maximal biomass concentrations and growth rates and by longer lag-phases. For example, the growth rate was reduced to half-maximal at 0.8 ± 0.0 g·L^{-1} xylitol and upon addition of 5 g·L^{-1} of xylitol, a lag-phase of 23 h was observed and the maximal biomass concentration was reduced by about threefold (Figure 3, Figure S1). A higher tolerance was observed with glucose as sole carbon source, e.g., a 20-times higher xylitol concentration (15.8 ± 0.1 g·L^{-1}) was required to reduce the growth rate to half maximal (Figure 3). Thus, while production of xylonate may either be coupled to growth or not, only growth-decoupled production may be a suitable strategy for a xylitol process.

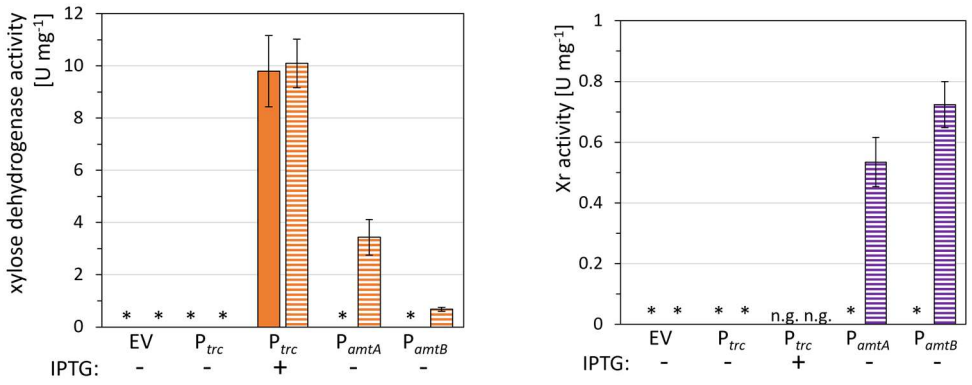

A **B**

Figure 2. Xylose dehydrogenase (**A**) and xylose reductase (**B**) activities in crude extracts of cells grown under nitrogen-rich or -limiting conditions. Cells of *C. glutamicum* gX derived strains for expression of *xylB* or *xr* from IPTG inducible P_{trc}, or nitrogen content-dependent P_{amtA} or P_{amtB} and the empty vector control strain gX-EV were grown in CgXII or N-CgXII, supplemented with 40 g·L^{-1} xylose for 68 h. For P_{trc}-controlled expression, 1 mM IPTG (+) was added at cultivation start. Values of means with standard deviations refer to at least three technical replicates. * = not detectable. (<0.05 U·mg^{-1}), n.g. = no growth.

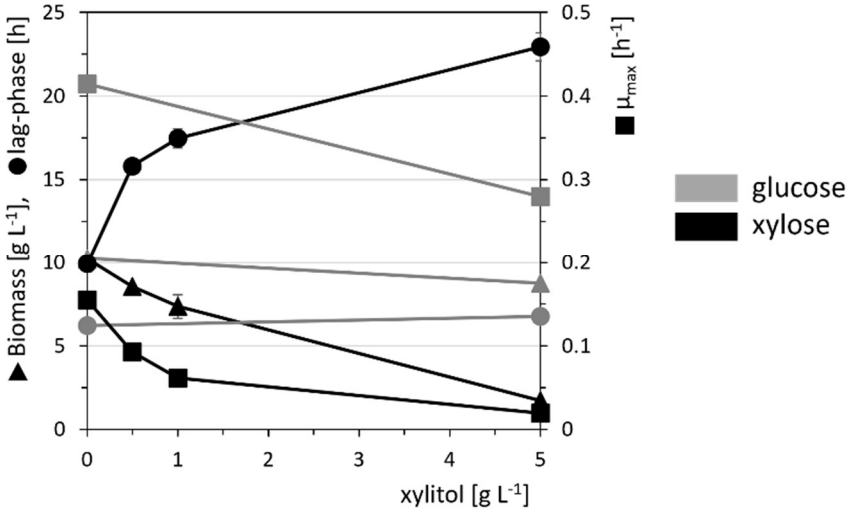

Figure 3. Effect of the addition of xylitol on growth of gX in CgXII medium with glucose (light grey) or xylose (black) as carbon sources. Biomass (triangles), maximal growth rates μ_{max} (squares) and lag-phases (circles) of cells grown in CgXII supplemented with 40 g·L^{-1} glucose (grey) or xylose (black) and 0–5 g·L^{-1} xylitol were determined in a BioLector microcultivation system during cultivation for 96 h. Values of means with standard deviations refer to triplicate cultivations.

3.4. Nitrogen-limitation Induced Production of the Sugar Acid Xylonate

Xylose functions as carbon and energy source for growth of *C. glutamicum* strain gX, and thus, production of xylonate or xylitol from xylose by this strain competes with biomass formation. Production can be decoupled from growth, e.g., by imposing a nutrition limitation other than xylose. Here, we used either medium CgXII with abundant nitrogen availability or medium N-CgXII with just 5% of the nitrogen content. *C. glutamicum* strains gX-EV and gX-P$_{trc}$-*xylB* were cultivated in CgXII and N-CgXII with 267 mM xylose. As expected, strain gX-EV did not produce xylonate. Without IPTG induction, strain gX-P$_{trc}$-*xylB* exhibited basal *xylB* expression that resulted in the maximal accumulation of approximately 90 mM xylonate after 72 h (Figure 4) irrespective of the nitrogen content in the cultivation medium (Table 3, Table S2). IPTG induction during inoculation increased xylonate production by strain gX-P$_{trc}$-*xylB* to 185 ± 13 after 72 h (Figure 4) and a maximum of 217 ± 7 mM after 144 h (Table 3, equivalent to 78 mol% of xylose oxidized to xylonate). This occurred at the cost of biomass formation that was diminished to about half (Figure 4 A; Table 3). Growth in the nitrogen-starvation medium N-CgXII was limited to reach a maximal biomass concentration of around 2.5 g·L^{-1} (Figure 4B,C) and strains gX-P$_{amtA}$-*xylB* and gX-P$_{amtB}$-*xylB* produced 209 ± 7 and 171 ± 9 mM xylonate, respectively, under these conditions (Table 3). Thus, about 77 and 63 mol% of xylose, respectively, was oxidized to xylonate. When nitrogen was abundant, both strains reached a higher biomass concentration (about 8 to 9 g·L^{-1}, Figure 4B,C) but accumulated less xylonate (about 50 mM, Table 3). As can be seen at the end of the culture (at 144 h; Table 3), the nitrogen-limitation induced xylonate production by the *C. glutamicum* strains gX-P$_{amtA}$-*xylB* and gX-P$_{amtB}$-*xylB* was comparable to IPTG-induced xylonate production by gX-P$_{trc}$-*xylB*. Notably, nitrogen-limitation induced xylonate production did not require addition of the costly inducer IPTG.

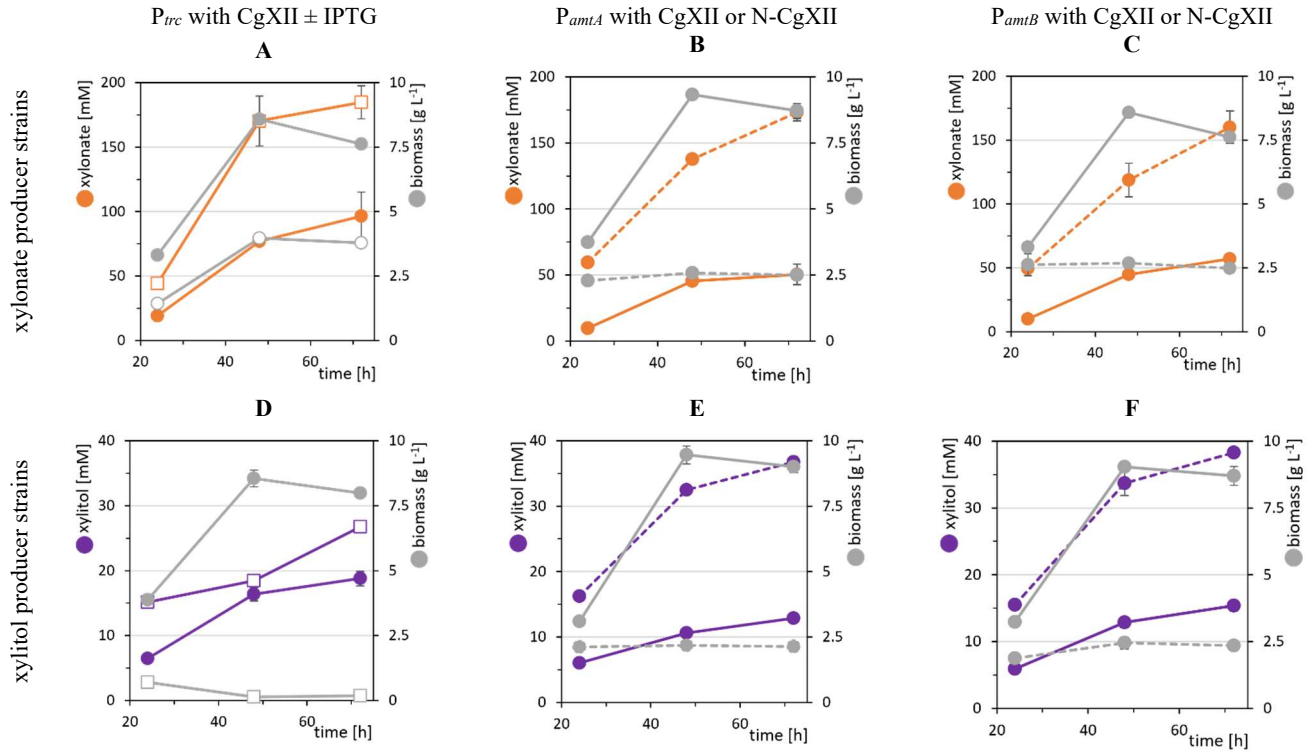

Figure 4. Biomass formation (grey) and production of xylonate (orange) or xylitol (purple) in xylose minimal medium. Strains gX-P$_{trc}$-*xylB* (**A**), gX-P$_{amtA}$-*xylB* (**B**), gX-P$_{amtB}$-*xylB* (**C**) gX-P$_{trc}$-*xr* (**D**), gX-P$_{amtA}$-*xr* (**E**), and gX-P$_{amtB}$-*xr* (**F**), were cultivated in CgXII (solid line) or N-CgXII (dashed line) supplemented with 40 g·L^{-1} xylose in shake flasks for 144 h. P$_{trc}$ was induced by addition of 1mM IPTG (open squares; **A**,**D**). Values of means with standard deviations refer to triplicate cultivations.

3.5. Nitrogen-limitation Induced Production of the Sugar Alcohol Xylitol

The previous finding that xylitol impaired growth suggested that its growth-decoupled production may be better than growth-associated production. In the absence of IPTG, strain gX-P$_{trc}$-*xr* utilized xylose completely, grew to a biomass concentration of 8.4 ± 0.2 g·L^{-1}, and due to leakage of the promoter P$_{trc}$, accumulated xylitol during growth and in the stationary phase until a final titer of 16 mM was reached (Figure 4D, Table 3). Induction with IPTG during inoculation abrogated growth, while 42 ± 4 mM xylitol accumulated and 191 ± 3 mM xylose remained in the broth, which is equivalent of 49 mol% conversion of xylose to xylitol (Table 3). With abundant nitrogen, strains gX-P$_{amtA}$-*xr* and gX-P$_{amtB}$-*xr* grew to biomass concentrations of around 9 g·L^{-1}, utilized xylose completely and produced 9 ± 1 mM and 13 ± 1 mM xylitol, respectively (Figure 4E,F; Table 3). Induction by nitrogen-limitation in medium N-CgXII considerably reduced biomass formation by strains gX-P$_{amtA}$-*xr* and gX-P$_{amtB}$-*xr* to around 2.5 g·L^{-1} and xylose utilization was incomplete as 104 ± 5 mM and 108 ± 10 mM xylose remained in the culture broth (Table 3). Notably, under these

conditions the highest final xylitol titers were observed: 86 ± 5 mM and 83 ± 10 mM xylitol (corresponding to conversion of 50 and 49 mol% of xylose, Table 3) for strains gX-P_{amtA}-*xr* and gX-P_{amtB}-*xr*, respectively, which was twofold higher than the xylitol titer obtained with the P_{trc} system (Table 3). Thus, nitrogen-limitation-induced xylitol production by the *C. glutamicum* strains gX-P_{amtA}-*xr* and gX-P_{amtB}-*xr* proved superior to the production via IPTG induction as addition of costly compounds for induction was not required and higher product titers were achieved.

Table 3. Biomass formation, product titers, and remaining xylose concentrations in cultivation using xylose minimal medium. Xylitol and xylonate producer strains gX-P_{amtA}-*xr*, gX-P_{amtB}-*xr*, gX-P_{amtA}-*xylB*, and gX-P_{amtB}-*xylB* were cultivated with 40 g·L^{-1} xylose in shake flasks for 144 h either with 100% nitrogen (CgXII) or with 5% nitrogen (N-CgXII). Strains gX-P_{trc}-*xr*, and gX-P_{trc}-*xylB* were cultivated in CgXII with/without IPTG induction of P_{trc}. Values of means with standard deviations refer to triplicate cultivations.

		Medium	Biomass [g·L^{-1}]	Product [mM]	Xylose [mM]
xylonate producer strains	gX-P_{trc}-*xylB*	CgXII	7.9 ± 0.1	86 ± 4	<1
		CgXII + IPTG	3.8 ± 0.1	217 ± 7	<1
	gX-P_{amtA}-*xylB*	CgXII	9.0 ± 0.4	53 ± 2	<1
		N-CgXII	2.6 ± 0.1	209 ± 7	5 ± 1
	gX-P_{amtB}-*xylB*	CgXII	9.0 ± 0.1	48 ± 4	<1
		N-CgXII	2.7 ± 0.2	171 ± 9	6 ± 1
xylitol producer strains	gX-P_{trc}-*xr*	CgXII	8.4 ± 0.2	16 ± 1	<1
		CgXII + IPTG	0.2 ± 0.1	42 ± 4	191 ± 3
	gX-P_{amtA}-*xr*	CgXII	8.9 ± 0.3	9 ± 1	<1
		N-CgXII	2.5 ± 0.2	86 ± 5	104 ± 5
	gX-P_{amtB}-*xr*	CgXII	9.1 ± 0.9	13 ± 1	<1
		N-CgXII	2.6 ± 0.2	83 ± 10	108 ± 10

4. Discussion and Conclusions

In this study, we exemplified the suitability of nitrogen limitation-inducible promoters as an efficient tool for inducer-free dynamic modulation of gene expression by induction or CRISPRi-mediated knockdown in *C. glutamicum*. This strategy, which does not require constant process monitoring, was successfully applied to the inducer-free production of two products derived from the lignocellulosic pentose sugar xylose. While production of the sugar acid xylonate reached comparable titers as production induced with the costly IPTG, production of the growth-inhibitory sugar alcohol xylitol outperformed IPTG-inducible xylitol product titers by a factor of about two. Thus, growth-decoupled production using the nitrogen-limitation-inducible promoters P_{amtA} and P_{amtB} proved to be particularly valuable for production of the growth-inhibitory product xylitol.

The production of growth-inhibitory products benefits from decoupling production from growth. Expression of the respective genes for the biosynthesis pathway has to be tightly controlled. Basal transcription from leaky induction systems like the classic IPTG inducible P_{trc} promoter often hampers the attainment of stable, scalable two-stage cultivation processes, that allow predictable scale-up and transfer to different cultivation systems and initiated versatile efforts for its diminution. The leakiness of the T7 promoter system was reduced by inhibiting transcription initiation by binding of the T7 lysozyme to T7 RNA polymerase [75]. Besides tight regulation with low leakiness, timing of expression is key to production of growth-inhibitory compounds. For example, an antibiotic may be added as shown for production of L-glutamic acid by *C. glutamicum* upon addition of the DNA gyrase inhibitor ciprofloxacin [76]. Alternatively, metabolic engineering made use of promoters that show expression only in the stationary growth phase as applied to fermentative production of the secondary metabolite lovastatin by the fungus *Aspergillus terreus* [77]. The medium formulation may be adjusted such that a macronutrient becomes limiting for growth, but growth-decoupled production continues. As most, if not all, products contain carbon atoms, carbon source limitation typically is not beneficial. Instead, a limiting P or N source may be used to decouple production from growth. However, the chosen products should lack either P or N atoms. Phosphate limitation-induced expression has been applied to production of recombinant proteins by *E. coli* [54]. Promoters of *E. coli*, activated by the transcriptional activator PhoB, were also used for xylitol production to a titer of 200 g·L^{-1} at 86 mol% conversion [78]. Although the nutrient starvation response is intrinsically subject to species- or strain-specific complex regulatory patterns, often rendering nutrient limitation-induced production too sensible for straight transfer [46], conserved regulatory mechanisms may make transfer to *C. glutamicum* possible since its phosphate starvation response is well characterized [79]. Recently, the choice of the nitrogen source and nitrogen catabolite repression have been exploited for production of glycosylated and secreted proteins by *Aspergillus nidulans* [53]. Based on the knowledge on the AmtR regulon [42], we have compared nitrogen-dependent promoters for induction of xylitol and xylonate biosynthesis genes and identified P_{amtA} and P_{amtB} applicable to precise expression control without the requirement for induction of costly inducers. Depending on the product and process, other promoters regulated by AmtR may prove better due to different promoter strengths or basal activities.

The xylonate titers achieved here with *C. glutamicum* gX-P_{amtA}-*xylB* (up to 34 ± 1.1 g·L^{-1} at 144 h, Table 3) are promising, but have to be optimized further for industrial application. For example, the nitrogen content has to be optimized further to realize the highest possible biomass concentration for subsequent use in non-growth associated production. Moreover, cultivation in fed-batch mode may be helpful to maintain non-growth associated production with the highest possible biomass concentration over

extended time periods. NAD^+-dependent xylose oxidation by XylB yields one reduction equivalent per xylonate produced. Under anaerobic conditions surplus NADH can easily be oxidized. An approach often chosen to improve xylonate titers is the addition of other carbon sources along with xylose and/or the addition of complex media components such as yeast extract [18,80]. The volumetric productivity may be improved by deletion of the gene for the transcriptional repressor IolR since the gene for the native myo-inositol 2-dehydrogenase (IolG, cg0204), which also oxidizes D-xylose, would be derepressed [81]. However, degradation of xylonate by the enzymes encoded in the *iol* operons [82] has to be abolished by deletion of the respective genes. Although hydrolysis of D-1,4-xylonolactone generated in the xylose dehydrogenase reaction is thought to occur spontaneously, the additional expression of the gene for D-1,4-xylonolactonase from *C. crescentus* may accelerate xylonate production. Enzyme catalysis is also known for biotransformation of xylose to xylonate. However, this requires redox cofactor regeneration which may be achieved by electrodialysis [83] and often suffers from enzyme instability. To overcome the latter, immobilization of xylose dehydrogenase on triglycine functionalized PEGylated gold nanoparticles via *C. glutamicum* sortase E improved enzyme stability as compared to free enzymes [84]. Since the product xylonate is an acid with a pKa of 3.56, enzyme catalysis, whole-cell biotransformation and fermentation have to be well-buffered, which may limit downstream processing. The latter may also be a challenge to use lignocellulosic hydrolysates that contain a notable fraction of xylose. Future work is required to see if industrial key performance indicators (KPIs) can be reached for xylonate production from xylose.

Likewise, xylitol production requires further optimization to achieve industrial KPIs. Although the xylitol titers achieved here were about an order of magnitude higher than those obtained previously with *C. glutamicum* (about 86 mM or 13 $g \cdot L^{-1}$ as compared to 1.1 $g \cdot L^{-1}$ [72]), Xr activity in crude extracts of nitrogen-starved gX cells only amounted to approximately 10% of that reported previously (0.53 ± 0.08 $U \cdot mg^{-1}$ and 0.72 ± 0.08 $U \cdot mg^{-1}$, Figure 3A, as compared to 6.4 ± 0.1 $U \cdot mg^{-1}$ [72]). Remarkably, the titer obtained here with strain gX-P_{amtA}-*xr* (13.0 ± 0.7 $g \cdot L^{-1}$, Table 3) exceeded the concentration that diminished growth to half maximum (Figure 2) by 15-fold. This clearly indicates the beneficial effect of decoupling xylitol production from growth. Xylitol related growth inhibition may be due to formation of xylitol 5-phosphate, which noncompetitively inhibits xylose transporters, by xylulokinase [74,85]. In this respect, it has to be noted that the gene for the endogenous xylulokinase (cg0147, $xylB_{C.g.}$) is overexpressed to enable utilization of xylose for growth. As way out, either native xylulokinase was be replaced by a D-xylulokinase variant from *Pichia stipitis* [85], which does not accept xylitol as substrate, or introduction of the oxidative Weimberg pathway for xylose utilization may help [86]. The inhibition by xylitol 5-phosphate formed during xylose utilization in our strains also occurs during xylonate production. However, here the xylitol titers achieved were two- to threefold lower when compared to the xylonate titers (about 86 mM xylitol in comparison to about 210 mM xylonate; Table 3). About 0.5 $mol \cdot mol^{-1}$ xylitol were produced from xylose (Table 3). Based on the degrees of reduction of xylose and xylitol a theoretical maximal yield of 0.91 $mol \cdot mol^{-1}$ can be calculated (as compared to 1.1 $mol \cdot mol^{-1}$ for xylonate). It has to be noted that reduction of xylose to xylitol requires NADPH. Thus, a fraction of xylose is used not only to form biomass, but also serves to provide NADPH for xylitol production. The complete oxidation of one molecule of xylose to five molecules of CO_2 yields 10 NADPH. Therefore, the maximal theoretical xylitol pathway yield from xylose is sub-stoichiometric at 0.83 $mol \cdot mol^{-1}$ [87]. However, NADPH formation may even be lower as NADH instead of NADPH may be formed during xylose oxidation. This may be alleviated by heterologous expression of the genes for the membrane-bound transhydrogenase PntAB from *E. coli* in order to convert NADH to NADPH [88]. Alternatively, glucose or gluconate was used as co-substrate to continuously replenish the NADPH pool during xylose reduction [26,72,78]. The use of mixtures of xylose and glucose may be relevant as both are the dominating sugars present in lignocellulosic hydrolysates.

Our demonstration of using nitrogen starvation promoters in different setups for gene expression or CRISPRi-mediated gene knockdown provides a promising foundation, transferable to other processes. Transfer to bioprocesses with *C. glutamicum* using carbon sources other than xylose appears straightforward. With regards to the product scope, applications involving growth-inhibitory intermediates or targeting products may be most beneficial for the type of growth-decoupled production developed here.

Supplementary Materials

Summarize the supplementary information with the caption names in this section. The following supporting information can be found at: https://www.sciepublish.com/index/journals/article_htm/sbe/25.html/id/46, Table S1: List of oligonucleotides used in this work.; Figure S1: Titers of xylitol or xylonate, produced by gX derived strains with P_{trc}, P_{amtA}, or P_{amtB}; Figure S2: Titers of xylitol or xylonate, produced by gX derived strains with P_{trc}, P_{amtA}, or P_{amtB}.

Acknowledgements

The authors gratefully acknowledge fruitful discussion with the whole ForceYield project team.

Author Contributions

V.F.W and L.S.S. conceptualized the study, M.R. and L.S.S. performed experiments, V.F.W. acquired funding, L.S.S. and V.F.W drafted the manuscript, all authors reviewed and approved the final manuscript.

Ethics Statement

Not applicable.

Informed Consent Statement

Not applicable.

Funding

This work was supported in part by the BMBF project ForceYield (031B0825C). The funders had no role in the design of the study, in the collection, analyses, or interpretation of data; in the writing of the manuscript or in the decision to publish the results.

Declaration of Competing Interest

The authors declare that they have no known competing financial interests or personal relationships that could have appeared to influence the work reported in this paper.

References

1. Dahmen N, Lewandowski I, Zibek S, Weidtmann A. Integrated lignocellulosic value chains in a growing bioeconomy: Status quo and perspectives. *GCB Bioenergy* **2019**, *11*, 107–117.
2. Gopinath V, Meiswinkel TM, Wendisch VF, Nampoothiri KM. Amino acid production from rice straw and wheat bran hydrolysates by recombinant pentose-utilizing *Corynebacterium glutamicum*. *Appl. Microbiol. Biotechnol.* **2011**, *92*, 985–996.
3. Kirimura K, Honda Y, Hattori T. Gluconic and Itaconic Acids. In *Comprehensive Biotechnology*, 2nd ed.; Moo-Young M, Ed.; Academic Press: Burlington, NJ, USA, 2011; pp. 143–147.
4. Toivari MH, Ruohonen L, Richard P, Penttilä M, Wiebe MG. *Saccharomyces cerevisiae* engineered to produce D-xylonate. *Appl. Microbiol. Biotechnol.* **2010**, *88*, 751–760.
5. Chun B-W; Dair B, Macuch PJ, Wiebe D, Porteneuve C, Jeknavorian A. The development of cement and concrete additive. *Appl. Biochem. Biotechnol.* **2006**, *131*, 645–658.
6. Millner OE, Clarke RP, Titus GR. Clarifiers for Polyolefins and Polyolefin Compositions Containing Same. US Patent US5302643A, 1994.
7. Zamora F, Bueno M, Molina I, Iribarren JI, Muñoz-Guerra S, Galbis JA. Stereoregular Copolyamides Derived from D-Xylose and L-Arabinose. *Macromolecules* **2000**, *33*, 2030–2038.
8. Markham RG. Compositions and Methods for Administering Therapeutically Active Compounds. US Patent US5070085A, 1991.
9. Niu W, Molefe MN, Frost JW. Microbial Synthesis of the Energetic Material Precursor 1,2,4-Butanetriol. *J. Am. Chem. Soc.* **2003**, *125*, 12998–12999.
10. Wang J, Shen X, Jain R, Wang J, Yuan Q, Yan Y. Establishing a novel biosynthetic pathway for the production of 3,4-dihydroxybutyric acid from xylose in *Escherichia coli*. *Metab. Eng.* **2017**, *41*, 39–45.
11. Governo AT, Proença L, Parpot P, Lopes MIS, Fonseca ITE. Electro-oxidation of D-xylose on platinum and gold electrodes in alkaline medium. *Electrochim. Acta* **2004**, *49*, 1535–1545.
12. Trichez D, Carneiro CVGC, Braga M, Almeida JRM. Recent progress in the microbial production of xylonic acid. *World J. Microbiol. Biotechnol.* **2022**, *38*, 127.
13. Buchert J, Viikari L, Linko M, Markkanen P. Production of xylonic acid by *Pseudomonas fragi*. *Biotechnol. Lett.* **1986**, *8*, 541–546.
14. Wang C, Wei D, Zhang Z, Wang D, Shi J, Kim CH, et al. Production of xylonic acid by *Klebsiella pneumoniae*. *Appl. Microbiol. Biotechnol.* **2016**, *100*, 10055–10063.
15. Bondar M, da Fonseca MMR, Cesário MT. Xylonic acid production from xylose by *Paraburkholderia sacchari*. *Biochem. Eng. J.* **2021**, *170*, 107982.
16. Buchert J, Puls J, Poutanen K. Comparison of *Pseudomonas fragi* and *Gluconobacter oxydans* for production of xylonic acid from hemicellulose hydrolyzates. *Appl. Microbiol. Biotechnol.* **1988**, *28*, 367–372.
17. Liu H, Valdehuesa KNG, Nisola GM, Ramos KRM, Chung W-J. High yield production of D-xylonic acid from D-xylose using engineered *Escherichia coli*. *Bioresour. Technol.* **2012**, *115*, 244–248.
18. Sundar MSL, Susmitha A, Rajan D, Hannibal S, Sasikumar K, Wendisch VF, et al. Heterologous expression of genes for bioconversion of xylose to xylonic acid in *Corynebacterium glutamicum* and optimization of the bioprocess. *AMB Express* **2020**, *10*, 68.
19. Karl T. Technology of Main Ingredients—Sweeteners and Lipids. In *The Technology of Wafers and Waffles I—Operational Aspects*, 1st ed.; Academic Press: Cambridge, MA, USA, 2017; pp. 123–225.
20. Mussatto SI. Application of xylitol in food formulations and benefits for health. In *D-Xylitol*, 1st ed.; Springer-Verlag: Berlin/Heidelberg, Germany, 2012; pp. 309–323.
21. Delgado Arcaño Y, Valmaña García OD, Mandelli D, Carvalho WA, Magalhães Pontes LA. Xylitol: A review on the progress and challenges of its production by chemical route. *Catal. Today* **2020**, *344*, 2–14.
22. Park Y-C, Oh EJ, Jo J-H, Jin Y-S, Seo J-H. Recent advances in biological production of sugar alcohols. *Curr. Opin. Biotechnol.* **2016**, *37*, 105–113.

23. Umai D, Kayalvizhi R, Kumar V, Jacob S. Xylitol: Bioproduction and Applications-A Review. *Front. Sustain.* **2022**, *3*, 826190.
24. Yoshitake J, Shimamura M, Imai T. Xylitol Production by a *Corynebacterium* Species. *Agric. Biol. Chem.* **1973**, *37*, 2251–2259.
25. Kumar V, Krishania M, Preet Sandhu P, Ahluwalia V, Gnansounou E, Sangwan RS. Efficient detoxification of corn cob hydrolysate with ion-exchange resins for enhanced xylitol production by *Candida tropicalis* MTCC 6192. *Biores. Technol.* **2018**, *251*, 416–419.
26. Sasaki M, Jojima T, Inui M, Yukawa H. Xylitol production by recombinant *Corynebacterium glutamicum* under oxygen deprivation. *Appl. Microbiol. Biotechnol.* **2010**, *86*, 1057–1066.
27. Wendisch VF. Metabolic engineering advances and prospects for amino acid production. *Metab. Eng.* **2020**, *58*, 17–34.
28. Lee J-H, Wendisch VF. Production of amino acids–Genetic and metabolic engineering approaches. *Biores. Technol.* **2017**, *245*, 1575–1587.
29. Sasaki M, Jojima T, Inui M, Yukawa H. Simultaneous utilization of D-cellobiose, D-glucose, and D-xylose by recombinant *Corynebacterium glutamicum* under oxygen-deprived conditions. *Appl. Microbiol. Biotechnol.* **2008**, *81*, 691–699.
30. Song Y, Matsumoto K, Yamada M, Gohda A, Brigham CJ, Sinskey AJ, et al. Engineered *Corynebacterium glutamicum* as an endotoxin-free platform strain for lactate-based polyester production. *Appl. Microbiol. Biotechnol.* **2012**, *93*, 1917–1925.
31. Wolf S, Becker J, Tsuge Y, Kawaguchi H, Kondo A, Marienhagen J, et al. Advances in metabolic engineering of *Corynebacterium glutamicum* to produce high-value active ingredients for food, feed, human health, and well-being. *Essays Biochem.* **2021**, *65*, 197–212.
32. Hu M, Liu F, Wang Z, Shao M, Xu M, Yang T, et al. Sustainable isomaltulose production in *Corynebacterium glutamicum* by engineering the thermostability of sucrose isomerase coupled with one-step simplified cell immobilization. *Front. Microbiol.* **2022**, *13*, 979079.
33. Shin K-C, Sim D-H, Seo M-J, Oh D-K. Increased Production of Food-Grade D-Tagatose from D-Galactose by Permeabilized and Immobilized Cells of *Corynebacterium glutamicum*, a GRAS Host, Expressing D-Galactose Isomerase from *Geobacillus thermodenitrificans*. *J. Agric. Food Chem.* **2016**, *64*, 8146–8153.
34. Shyamkumar R, Moorthy IG, Ponmurugan K, Baskar R. Production of L-glutamic Acid with *Corynebacterium glutamicum* (NCIM 2168) and *Pseudomonas reptilivora* (NCIM 2598): A Study on Immobilization and Reusability. *Avicenna J. Med. Biotechnol.* **2014**, *6*, 163–168.
35. Tsuge Y, Matsuzawa H. Recent progress in production of amino acid-derived chemicals using *Corynebacterium glutamicum*. *World J. Microbiol. Biotechnol.* **2021**, *37*, 49.
36. Wördemann R, Wiefel L, Wendisch VF, Steinbüchel A. Incorporation of alternative amino acids into cyanophycin by different cyanophycin synthetases heterologously expressed in *Corynebacterium glutamicum*. *AMB Express* **2021**, *11*, 55.
37. Becker J, Wittmann C. Diamines for Bio-Based Materials. In *Industrial Biotechnology: Products and Processes*; Wiley-VCH: Weinheim, Germany, 2016; pp. 391–409.
38. Hüser AT, Chassagnole C, Lindley ND, Merkamm M, Guyonvarch A, Elisáková V, et al. Rational design of a *Corynebacterium glutamicum* pantothenate production strain and its characterization by metabolic flux analysis and genome-wide transcriptional profiling. *Appl. Environ. Microbiol.* **2005**, *71*, 3255–3268.
39. Wieschalka S, Blombach B, Bott M, Eikmanns BJ. Bio-based production of organic acids with *Corynebacterium glutamicum*. *Microb. Biotechnol.* **2013**, *6*, 87–102.
40. Inui M, Kawaguchi H, Murakami S, Vertes A, Yukawa H. Metabolic Engineering of *Corynebacterium glutamicum* for Fuel Ethanol Production under Oxygen-Deprivation Conditions. *J. Mol. Microbiol. Biotechnol.* **2004**, *8*, 243–254.
41. Zahoor A, Lindner SN, Wendisch VF. Metabolic engineering of *Corynebacterium glutamicum* aimed at alternative carbon sources and new products. *Comput. Struct. Biotechnol. J.* **2012**, *3*, e201210004.
42. Jakoby M, Nolden L, Meier-Wagner J, Krämer R, Burkovski A. AmtR, a global repressor in the nitrogen regulation system of *Corynebacterium glutamicum*. *Mol. Microbiol.* **2000**, *37*, 964–977.
43. Beckers G, Strösser J, Hildebrandt U, Kalinowski J, Farwick M, Krämer R, et al. Regulation of AmtR-controlled gene expression in *Corynebacterium glutamicum*: mechanism and characterization of the AmtR regulon. *Mol. Microbiol.* **2005**, *58*, 580–595.
44. Taylor ND, Garruss AS, Moretti R, Chan S, Arbing MA, Cascio D, et al. Engineering an allosteric transcription factor to respond to new ligands. *Nat. Methods* **2016**, *13*, 177–183.
45. Briand L, Marcion G, Kriznik A, Heydel JM, Artur Y, Garrido C, et al. A self-inducible heterologous protein expression system in *Escherichia coli*. *Sci. Rep.* **2016**, *6*, 33037.
46. Chubukov V, Sauer U. Environmental Dependence of Stationary-Phase Metabolism in *Bacillus subtilis* and *Escherichia coli*. *Appl. Environ. Microbiol.* **2014**, *80*, 2901–2909.
47. Burg JM, Cooper CB, Ye Z, Reed BR, Moreb EA, Lynch MD. Large-scale bioprocess competitiveness: the potential of dynamic metabolic control in two-stage fermentations. *Curr. Opin. Chem. Eng.* **2016**, *14*, 121–136.
48. Choudhary S, Schmidt-Dannert C. Applications of quorum sensing in biotechnology. *Appl. Microbiol. Biotechnol.* **2010**, *86*, 1267–1279.
49. Stülke J, Hillen W. Carbon catabolite repression in bacteria. *Curr. Opin. Microbiol.* **1999**, *2*, 195–201.
50. Studier FW. Protein production by auto-induction in high density shaking cultures. *Protein Expr. Purif.* **2005**, *41*, 207–234.
51. Studier FW. Stable expression clones and auto-induction for protein production in *E. coli*. In *Structural Genomics*; Springer Nature: Berlin, Germany, 2014; Volume 1091.
52. Tahara N, Tachibana I, Takeo K, Yamashita S, Shimada A, Hashimoto M, et al. Boosting Auto-Induction of Recombinant Proteins in *Escherichia coli* with Glucose and Lactose Additives. *Protein Pept. Lett.* **2021**, *28*, 1180–1190.

53. Yan Q, Han L, Liu X, You C, Zhou S, Zhou Z. Development of an auto-inducible expression system by nitrogen sources switching based on the nitrogen catabolite repression regulation. *Microb. Cell Fact.* **2022**, *21*, 73.
54. Huber R, Roth S, Rahmen N, Büchs J. Utilizing high-throughput experimentation to enhance specific productivity of an *E. coli* T7 expression system by phosphate limitation. *BMC Biotechnol.* **2011**, *11*, 22.
55. Hanahan D. Studies on transformation of *Escherichia coli* with plasmids. *J. Mol. Biol.* **1983**, *166*, 557–580.
56. Eggeling L, Bott M. *Handbook of Corynebacterium glutamicum*, 1st ed.; CRC Press: Boca Raton, FL, USA, 2005.
57. Kalinowski J, Bathe B, Bartels D, Bischoff N, Bott M, Burkovski A, et al. The complete *Corynebacterium glutamicum* ATCC 13032 genome sequence and its impact on the production of L-aspartate-derived amino acids and vitamins. *J. Biotechnol.* **2003**, *104*, 5–25.
58. Henke NA, Krahn I, Wendisch VF. Improved Plasmid-Based Inducible and Constitutive Gene Expression in *Corynebacterium glutamicum*. *Microorganisms* **2021**, *9*, 204.
59. Werner F, Schwardmann LS, Siebert D, Rückert-Reed C, Kalinowski J, Wirth M, et al. Metabolic engineering of *C. glutamicum* for fatty alcohol production from glucose and wheat straw hydrolysate. In *Advances in Lignocellulosic Biofuel Production Systems*; Woodhead Publishing: Sawston, UK, 2023.
60. Schäfer A, Tauch A, Jäger W, Kalinowski J, Thierbach G, Pühler A. Small mobilizable multi-purpose cloning vectors derived from the *Escherichia coli* plasmids pK18 and pK19: selection of defined deletions in the chromosome of *Corynebacterium glutamicum*. *Gene* **1994**, *145*, 69–73.
61. Kirchner O, Tauch A. Tools for genetic engineering in the amino acid-producing bacterium *Corynebacterium glutamicum*. *J. Biotechnol.* **2003**, *104*, 287–299.
62. Göttl V, Schmitt I, Braun K, Peters-Wendisch P, Wendisch VF, Henke NA. CRISPRi-library guided target identification for engineering carotenoid production by *Corynebacterium glutamicum*. *Microorganisms* **2021**, *9*, 670.
63. Eikmanns BJ, Thum-Schmitz N, Eggeling L, Lüdtke K-U, Sahm H. Nucleotide sequence, expression and transcriptional analysis of the *Corynebacterium glutamicum gltA* gene encoding citrate synthase. *Microbiology* **1994**, *140*, 1817–1828.
64. Cetnar DP, Salis HM. Systematic Quantification of Sequence and Structural Determinants Controlling mRNA stability in Bacterial Operons. *ACS Synth. Biol.* **2021**, *10*, 318–332.
65. Blin K, Pedersen LE, Weber T, Lee SY. CRISPy-web: An online resource to design sgRNAs for CRISPR applications. *Synth. Syst. Biotechnol.* **2016**, *1*, 118–121.
66. Gibson DG, Young L, Chuang R-Y, Venter JC, Hutchison CA, Smith HO. Enzymatic assembly of DNA molecules up to several hundred kilobases. *Nat. Methods* **2009**, *6*, 343–345.
67. Sambrook J, Fritsch EF, Maniatis T. *Molecular Cloning: A Laboratory Manual*, 2nd ed.; Cold Spring Harbor Laboratory Press: New York, NY, USA, 1989.
68. Bradford MM. A rapid and sensitive method for the quantitation of microgram quantities of protein utilizing the principle of protein-dye binding. *Anal. Biochem.* **1976**, *72*, 248–254.
69. Sánchez-Moreno I, Benito-Arenas R, Montero-Calle P, Hermida C, García-Junceda E, Fernández-Mayoralas A. Simple and Practical Multigram Synthesis of d-Xylonate Using a Recombinant Xylose Dehydrogenase. *ACS Omega* **2019**, *4*, 10593–10598.
70. Cleto S, Jensen JV, Wendisch VF, Lu TK. *Corynebacterium glutamicum* Metabolic Engineering with CRISPR Interference (CRISPRi). *ACS Synth. Biol.* **2016**, *5*, 375–385.
71. Tombolini R, Unge A, Davey ME, de Bruijn FJ, Jansson JK. Flow cytometric and microscopic analysis of GFP-tagged *Pseudomonas fluorescens* bacteria. *FEMS Microbiol. Ecol.* **1997**, *22*, 17–28.
72. Dhar KS, Wendisch VF, Nampoothiri KM. Engineering of *Corynebacterium glutamicum* for xylitol production from lignocellulosic pentose sugars. *J. Biotechnol.* **2016**, *230*, 63–71.
73. Meiswinkel TM, Gopinath V, Lindner SN, Nampoothiri KM, Wendisch VF. Accelerated pentose utilization by *Corynebacterium glutamicum* for accelerated production of lysine, glutamate, ornithine and putrescine. *Microb. Biotechnol.* **2013**, *6*, 131–140.
74. Radek A, Müller M-F, Gätgens J, Eggeling L, Krumbach K, Marienhagen J, et al. Formation of xylitol and xylitol-5-phosphate and its impact on growth of d-xylose-utilizing *Corynebacterium glutamicum* strains. *J. Biotechnol.* **2016**, *231*, 160–166.
75. Stano NM, Patel SS. T7 lysozyme represses T7 RNA polymerase transcription by destabilizing the open complex during initiation. *J. Biol. Chem.* **2004**, *279*, 16136–16143.
76. Lubitz D, Wendisch VF. Ciprofloxacin triggered glutamate production by *Corynebacterium glutamicum*. *BMC Microbiol.* **2016**, *16*, 235.
77. Askenazi M, Driggers EM, Holtzman DA, Norman TC, Iverson S, Zimmer DP, et al. Integrating transcriptional and metabolite profiles to direct the engineering of lovastatin-producing fungal strains. *Nat. Biotechnol.* **2003**, *21*, 150–156.
78. Li S, Ye Z, Moreb EA, Hennigan JN, Castellanos DB, Yang T, et al. Dynamic control over feedback regulatory mechanisms improves NADPH flux and xylitol biosynthesis in engineered *E. coli*. *Metab. Eng.* **2021**, *64*, 26–40.
79. Wendisch VF, Bott M. Phosphorus Metabolism and its Regulation. In *Corynebacteria: Genomics and Molecular Biology*, 1st ed, Ed.; Caister Academic Press: Poole, UK, 2008; pp. 203–216.
80. Yim SS, Choi JW, Lee SH, Jeon EJ, Chung W-J, Jeong KJ. Engineering of *Corynebacterium glutamicum* for Consolidated Conversion of Hemicellulosic Biomass into Xylonic Acid. *Biotechnol. J.* **2017**, *12*, 1700040.

81. Tenhaef N, Brüsseler C, Radek A, Hilmes R, Unrean P, Marienhagen J, Noack S. Production of d-xylonic acid using a non-recombinant *Corynebacterium glutamicum* strain. *Bioresour. Technol.* **2018**, *268*, 332–339.
82. Krings E, Krumbach K, Bathe B, Kelle R, Wendisch VF, Sahm H, et al. Characterization of myo-Inositol Utilization by *Corynebacterium glutamicum*: the Stimulon, Identification of Transporters, and Influence on L-Lysine Formation. *J. Bacteriol.* **2006**, *188*, 8054–8061.
83. Zhou X, Han J, Xu Y. Electrodialytic bioproduction of xylonic acid in a bioreactor of supplied-oxygen intensification by using immobilized whole-cell *Gluconobacter oxydans* as biocatalyst. *Bioresour. Technol.* **2019**, *282*, 378–383.
84. Susmitha A, Arya JS, Sundar L, Maiti KK, Nampoothiri KM. Sortase E-mediated site-specific immobilization of green fluorescent protein and xylose dehydrogenase on gold nanoparticles. *J. Biotechnol.* **2023**, *367*, 11–19.
85. Akinterinwa O, Cirino PC. Heterologous expression of d-xylulokinase from *Pichia stipitis* enables high levels of xylitol production by engineered *Escherichia coli* growing on xylose. *Metab. Eng.* **2009**, *11*, 48–55.
86. Tenhaef N, Kappelmann J, Eich A, Weiske M, Brieß L, Brüsseler C, et al. Microaerobic growth-decoupled production of α-ketoglutarate and succinate from xylose in a one-pot process using *Corynebacterium glutamicum*. *Biotechnol. J.* **2021**, *16*, 2100043.
87. Dugar D, Stephanopoulos G. Relative potential of biosynthetic pathways for biofuels and bio-based products. *Nat. Biotechnol.* **2011**, *29*, 1074–1078.
88. Kabus A, Georgi T, Wendisch VF, Bott M. Expression of the *Escherichia coli pntAB* genes encoding a membrane-bound transhydrogenase in *Corynebacterium glutamicum* improves L-lysine formation. *Appl. Microbiol. Biotechnol.* **2007**, *75*, 47–53.